High-resolution imaging of closely space objects with high contrast ratios

Douglas A. Hope[1,2], Stuart M. Jefferies[1,3], Gianluca Li Causi[4,6], Marco Stangalini[5,6], Fernando Pedichini[6,7], Massimiliano Mattioli[6,7], Simone Antoniucci[6,7], Vincenzo Testa[6,7], and Roberto Piazzesi[6,7]

[1] *Georgia State University, Atlanta, GA, USA*
[2] *Hope Scientific Renaissance, Colorado Springs, CO, USA*
[3] *University of Hawaii, Pukalani, HI, USA*
[4] *INAF-IAPS, Via del Fosso del Cavaliere, 100, 00133 Roma, Italy*
[5] *ASI Italian Space Agency, Via del Politecnico 33, 00133, Rome, Italy*
[6] *INAF-OAR National Institute for Astrophysics, Via Frascati 33, 00078 Monte Porzio Catone (RM), Italy*
[7] *INAF-ADONI, Adaptive Optics National Laboratory, Italy and INAF-ADONI, Adaptive Optics National Laboratory, Italy*

Compiled September 20, 2019

We show that the image restoration technique of multi-frame blind deconvolution (MFBD) is able to perform accurate modeling of the uncompensated speckle structure in an adaptive optics (AO) compensated image. This opens the door for detecting very faint objects close to bright sources, like extra-solar planets or debris next to artificial satellites. If sufficient rotation of the field-of-view is available, as in minutes-long acquisitions of astronomical targets, the MFBD technique can be used in conjunction with the angular differential imaging (ADI) technique, which is able to remove any subtle stationary residual present in the MFBD modeling of the speckle structure, for improved detection sensitivity. Using this MFBD-ADI approach we achieve a detection performance that is x5 better than the current state-of-the-art methods, ADI, principal component analysis, and speckle-free ADI, and we recover secondary targets with a contrast of 10^{-4} of the main target. If no field-of-view rotation is available, as in very short (a few seconds) image sequences, the standard ADI and principal component analysis methods cannot be used. Here the MFBD method is able to recover secondary targets with a contrast of 5 x 10^{-4}, which is commensurate with the performance of the current state-of-the-art techniques that are used when dealing with a static field-of-view: recurrence quantification analysis and speckle-free imaging.

http://dx.doi.org/10.1364/ao.XX.XXXXXX

1. INTRODUCTION

The monitoring and protection of satellites is a crucial component of national security and space traffic management. Characterizing the local space environment around important satellites, such as persistence surveillance platforms and communication satellites, requires an ability to robustly detect, identify and classify any objects or debris in proximity to the satellite that may pose a threat. Accomplishing this task requires using large aperture (>3m) ground-based telescopes. However, image blur caused by the finite aperture size of the telescope and dynamic atmospheric blur will cause the observed reflected solar illumination of the satellite to be smeared out across the image, effectively obscuring the presence of any faint object in proximity to the spacecraft.

Overcoming this problem of detecting a faint source embedded in the noise of another source, commonly referred to as the problem of identifying closely spaced objects (CSOs), requires both high-resolution and high-contrast imaging. The significant technical barrier that must be overcome is the removal of the image blur due to atmospheric turbulence. One step in overcoming this barrier is to equip the telescope with an AO system whose temporal response is matched to the Greenwood frequency of the site. However, even with such a system, the limited number of actuators on the deformable mirror are unable to correct the high spatial frequencies in the distorted wave front, thus limiting the effectiveness of the AO correction. This results in a residual blur in the image, due to the accumulation of uncorrected faint speckle structure in the point spread function (PSF), which can obscure the presence of any objects or debris near the primary satellite.

Using ground-based imagery of the heavens to resolve closely spaced objects that have high contrast ratios is also a challenge met by astronomers in their quest to image exoplanets in prox-

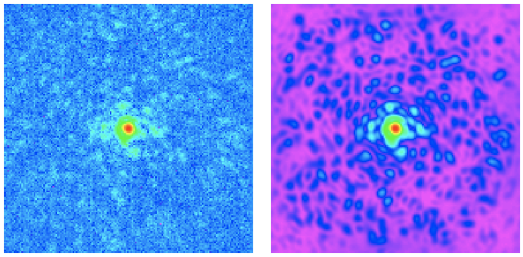

Fig. 1. An example data frame (left) and model from MFBD restoration of the 2,000-frame data set (right).

imity to their host stars. Indeed, significant research has been performed in this area and a number of techniques have been developed to extract faint signals from noisy backgrounds. These include angular differential imaging (ADI [8]), speckle-free angular differential imaging (SFADI [7]), incremental principal component analysis (iPCA [10]), and recurrence quantification analysis (RQA [4]). These approaches are able to detect CSOs with a typical contrast ratio of a few 10^{-4} in a 2-second sequence of data acquired at 1 kHz at visible wavelengths.

Here we investigate removing the residual blur in the AO-compensated imagery using numerical post processing. In particular, we look at the performance of the MFBD algorithm of Hope et al ([1]) for a single aperture. We then analyze the MFBD-restored data using the ADI technique to evaluate the performance of the MFBD algorithm on real on-sky acquisitions of an astronomical target. We refer to this approach as MFBD-ADI.

2. THE DATA

To investigate the potential performance of MFBD-ADI for the detection of CSOs, where one component is significantly fainter than the other, we use a series of images of the star Gliese 777 (magnitude +5.73). The images were acquired at a 1 ms cadence with the SHARK-VIS forerunner experiment [2] at the Large Binocular Telescope (LBT) in June, 2015. The observations were made through a 40 nm FWHM filter centered at 630 nm. The pixel scale on the camera was set at 3.73 mas providing a field-of-view of 0.61 arcsec x 0.61 arcsec. Images were acquired at high cadence by means of a sCMOS Andor Zyla imager with a typical read out noise of 1.36 e- per sample per pixel. The total duration of the data series was 20 min (or equivalently $1.2x10^6$ images), although here we only make use of a sub-set of 2,000 sequential images (2 s). During the frame acquisition, the LBT AO system was correcting 500 modes in closed loop, and seeing was in the range 0.9 - 1.2 arcsec giving an average atmospheric coherence length, r_0, of around 12 cm. If we assume the mean height for the turbulence is less than 20 km (almost certainly true), then this gives an isoplanatic angle that is greater than 0.78 arcsec. Since the field-of-view of our images is less than, or commensurate with, the isoplanatic angle for the observations, the use of the isoplanatic imaging equation to model the data in the MFBD algorithm is justified.

To estimate the performance of our MFBD-ADI technique for the detection of faint objects in proximity to a bright object, we injected synthetic sources into the real images, by re-scaling the PSF of the central object and adding photon noise with Poisson statistics, finally we imposed a field rotation of 30 degrees to the fake sources to mimic a typical high-elevation astronomical acquisition and to allow the use of Angular Differential Imaging post processing techniques. This approach for the assessment of a post-processing technique in high-contrast imaging has been used before [3]. These synthetic sources were scaled to have intensities of $5x10^{-4}$ and 10^{-4} of the intensities of the real images at distances between 100 mas to 300 mas from the bright central star. We note that using 2,000 frames to cover a field rotation of 30 degrees is equivalent to observing the host star for 30 minutes at ten degrees zenith angle from a medium latitude site, and using a sub-set of the frames equally spaced across the observing period for the analysis. We do this in order to simulate, with much less computational effort, the ADI processing that we will have when a full 120 minutes observation will be processed with MFBD.

We note that as the faint sources were injected with Poisson statistics, *not all the frames contain photons at the location of the maximum of the injected source itself* (given that the star has 1400 photons per frame on average in the central pixel), as expected in the real case at very high frame rates (i.e. 1 KHz) .

Figure (1) shows an example of a calibrated raw image.

3. RESULTS

We used a set of 2,000 frames of the SHARK data in a single MFBD restoration. This means that we need to determine approximately $5x10^7$ variables in order to model the data set. To avoid entrapment in local minima, we use a CMFBD approach to provide the initial estimates for the variables [5, 6]. We note that the data from the wave front sensor in the AO system were not available to help constrain the MFBD restoration.

Figure (1) shows an example of a model of a data frame and figure (2) shows the results of the MFBD-ADI analysis along with the iPCA, SFADI, and ADI approaches to the analysis. As can be seen, the MFBD-ADI technique is the *only* approach that can detect the signals at the 10^{-4} level. We note that the RQA approach performs similarly to the iPCA, SFADI and ADI techniques [4].

In order to assess how far we are from achieving the theoretical limit imposed by photon-noise plus detector-noise only, we simulated an ADI recovery for zero speckle noise (i.e. zero diversity in the speckle morphology). Basically, we generated a data cube of image frames where the image in each frame is equal to the average model plus its photon noise and read-out noise for the detector, and we injected the same 10^{-4} and $5x10^{-4}$ synthetic planets into the data cube, as done for the real sequence. In this way the standard ADI technique perfectly subtracts the fixed shape of the star. The result is an image of the "planets" that we would obtain if the speckles were "perfectly" removed from each frame, i.e. the noise limit. A comparison of the theoretical limit image with that from MFBD-ADI processing (see Figure (3)) shows that they are very similar. **That is, the MFBD-ADI result is very close to the theoretical noise limit!** We note that there is some margin for improvement, the r.m.s. of the background signal is 0.45 for MFBD-AD and 0.35 for noise limit; we are also investigating the potential of the ADI-based techniques when using ultra low noise detectors such as EM-CCDs that have a read out noise factor that is ten times lower than the 1.36 e- per sample per pixel of the Andor Zyla sCMOS camera used for the observations reported on here. The measured fluxes for the signals are shown in Table 1. This table compares the measured flux values for the MFBD-ADI recovery of the six injected "planets" to their true fluxes. The fluxes, top to bottom, correspond to the "planets" in the right-hand image in Figure (3) from top right

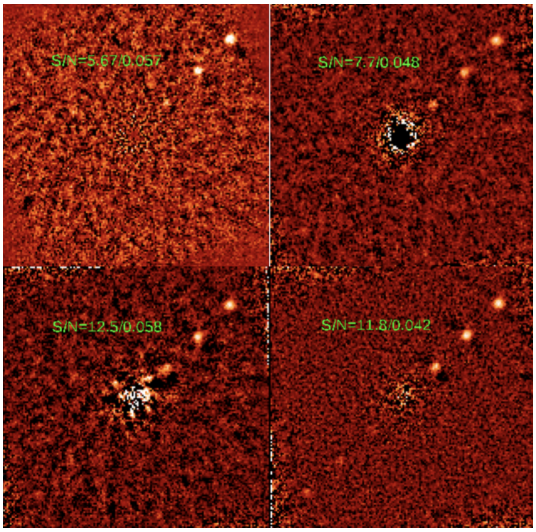

Fig. 2. Results from four different analysis techniques: iPCA (top left), SFADI (top right), ADI (bottom left), MFBD-ADI (bottom right). Note that MFBD-ADI is the only technique that detects the 3 injected signals at the 10^{-4} level (bottom left quadrant of image).

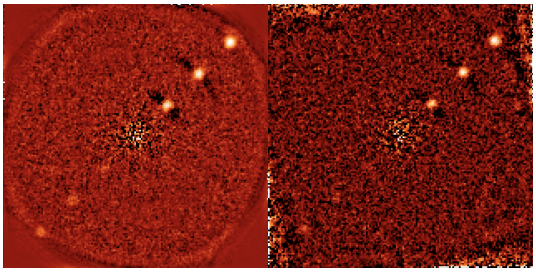

Fig. 3. ADI recovery for zero speckle noise, i.e. the noise limit (left), MFBD-ADI recovery (right). Note that the two recoveries are very similar.

to bottom left, respectively. We note that the observed small flux attenuation is normal with the ADI technique and can be accounted for with more complex photometric methods (e.g., the negative fake companion technique [9]).

Our results show that the MFBD algorithm of Hope et al. [1] provides high-fidelity modeling of the speckle structure in ground-based images of astronomical targets that arises from viewing through atmospheric turbulence. Moreover, when used in combination with angular differential imaging it provides a viable technique (MFBD-ADI) for resolving closely spaced objects with high contrast ratios for targets where there is significant field rotation during the observations (e.g., exoplanet systems and their host stars). We note that the 5x gain in sensitivity demonstrated here should allow the detection of planets down to 4x10^{-6} in the full 1.2 million frame sequence of the Forerunner observations (for which the SFADI technique reached 10^{-5} [7]).

Now the minimum field rotation for ADI-based techniques is the minimum angle,θ_{min}, which avoids self-subtraction, that is, the angle subtended by one or two full-width at half maximum

Table 1. Photometry for MFBD-AD Analysis

measured flux	true flux	contrast
13.4 ± 4.4	18.2	5e-4
11.8 ± 4.1		
7.7 ± 3.3		
1.7 ± 1.6	3.65	1e-4
2.3 ± 1.8		
2.8 ± 2.0		

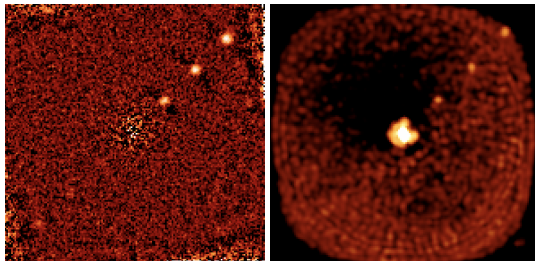

Fig. 4. Recovery from data with field rotation (left) and without field rotation (right). Note, the right-hand image shows the central star, which is saturated in order to show the detection of the 5 x 10^{-4} signals in the upper right quadrant. The origin of the subtle ringing artifact in the right-hand image (seen near the bottom edge) needs to be tracked down before we can expect to detect the 10^{-4} signals.

(FWHM) of the PSF at the planet's separation from the star:

$$\theta_{min} = \arctan(\text{FWHM}/\text{separation}). \quad \textbf{(1)}$$

If the rotation of the field-of-view is smaller than this, the median stack of the frames will contain some of the planet's information because the planet stays in the same position, within one or two FWHM. Therefore, of course, the minimum angle for ADI analysis decreases with separation. So, what about CSOs with high-contrast ratios where there is field rotation that is less than, or commensurate with, θ_{min}?

To evaluate the limiting case of no field rotation, we look at the contrast that we can achieve using only MFBD and 2,000 frames of data where there is no field rotation. That is, this time we look at a data set where the "planets" are injected without field rotation. The results, which are shown in Figure 4, indicate that we can achieve a contrast of 5e^{-4} using only MFBD for the processing of a 2-second sequence of data acquired at 1 kHz with only a slight decrease of the signal-to-noise ratio with respect to the MFBD-ADI result.

4. SUMMARY

We have shown that MFBD is able to perform accurate modeling of the structure in a speckle image. This opens the door for detecting very faint objects close to bright sources, like extra-solar planets or debris next to artificial satellites. If sufficient rotation of the field-of-view is available, as in minutes-long acquisitions of astronomical targets, the MFBD technique can be used in conjunction with the ADI technique, which is able to remove any subtle stationary residual present in the MFBD modeling of the

speckle structure, for improved detection sensitivity. Using this MFBD-ADI approach we achieve a detection performance that is x5 better than the current state-of-the-art methods, ADI, iPCA, and SFADI, and we recover secondary targets with a contrast of 10^{-4} of the main target. If no field-of-view rotation is available, as in very short (a few seconds) image sequences, the standard ADI and PCA cannot be used. Here MFBD is able to recover secondary targets with a contrast of 5 x 10^{-4}, which is commensurate with the performance of the current state-of-the-art techniques that are used when dealing with a static field-of-view: RQA and speckle-free imaging [4]. We are working on removing the subtle ringing effect that appears in the MFBD modeling of the speckle data for the static field-of-view case (this effect is automatically subtracted out in the case of MFBD-ADI).

Lastly, we note that this research has implications for imaging satellites in geosynchronous orbit with 3m-class telescopes, and looking for debris or small pico-scale satellites in proximity. As targets in geosynchronous orbit (GEO) describe a "figure of eight" (an analemma) in the sky, which is extremely small for a "geostationary" satellites, we are interested in the "no field rotation" results presented above. With a 3m-class telescope, satellites in GEO are essentially unresolved and thus the techniques discussed above are pertinent. However, these satellites have an average brightness of around magnitude +11, which makes them extremely faint. To study the performance of the MFBD technique presented here for such faint targets, we have acquired observations of a magnitude +9 star with an orbiting planet. We will present the results of the analysis of these data at a future AMOS conference.

5. FUNDING INFORMATION

The Air Force Office of Scientific Research funded DAH and SMJ's contributions to this work through contract FA9550-14-1-0178.

REFERENCES

1. D. Hope, S. M. Jefferies, M. Hart, and J. Nagy, *High-resolution speckle imaging through strong atmospheric turbulence*, Optics Express, 24, 12116-12129, 2016.
2. F. Pedichini, M. Stangalini, F. Ambrosino, A. Puglisi, E. Pinna, V. Bailey, L. Carbonaro, M. Centrone, J. Christou, S. Esposito, J. Farinato, F. Fiore1, E. Giallongo, J. M. Hill, P. M. Hinz, and and L. Sabatini, The Astronomical Journal, 154, 74-78, 2017.
3. A. Amara and S. P. Quanz, *PYNPOINT: An image processing package for finding exoplanets*, Monthly Notices of the Royal Astronomical Society, 427, 948, 2012.
4. M. Stangalini, G. Li Causi, F. Pedichini, S. Antoniucci, M. Mattioli, J. Christou, G. Consolini, D. Hope, S. M. Jefferies, R. Piazzesi, and V. Testa, *Recurrence quantification analysis as a post-processing technique in adaptive optics high-contrast imaging*, The Astrophysical Journal, 868:6, 2018.
5. D. A. Hope and S. M. Jefferies, *Compact multi-frame blind deconvolution*, Optics Letters, 36, 867-869, 2011.
6. D. A. Hope, S. M.Jefferies, and C. Smith, *High-fidelity imaging using compact multi-frame blind deconvolution*, Journal Astronautical Science, 1-8, 2019.
7. G. Li Causi, M. Stangalini, S. Antoniucci, et al. The Astrophysical Journal, 849, 85, 2017
8. C. Marois, D. Lafreni'ere, D., R. Doyon, B. Macintosh, and D. Nadeau, The Astrophysical Journal, 641, 556-564, 2006.
9. C. A. Gomez Gonzalez, O. Wertz, O. Absil, V. Christiaens, D. Defrere, D. Mawet, J. Milli, P.-A. Absil, M. Van Droogenbroeck, F. Cantalloube, P. M. Hinz, A. J. Skemer, M. Karlsson, J. Surdej, arXiv: 1705.06184v1, 17 May 2017
10. D. Ross, J. Lim, R. Lin, M. Yang. Incremental Learning for Robust Visual Tracking, International Journal of Computer Vision, Volume 77, Issue 1-3, pp. 125-141, May 2008